Three-dimensional-printed membrane-type acoustic metamaterial for low frequency sound attenuation

Alexandre Leblanc, Antoine Lavie

Alexandre Leblanc and Antoine Lavie: JASA Express Letters [http://dx.doi.org/10.1121/1.4984623] Published Online 9 June 2017

Three-dimensional-printed membrane-type acoustic metamaterial for low frequency sound attenuation

Alexandre Leblanc[a] **and Antoine Lavie**
Univ. Artois, Ecole des Mines, Fédération Universitaire et Polytechnique de Lille, Univ. Lille, EA 4515, Laboratoire de Génie Civil et géo-Environnement (LGCgE), F-62400 Béthune, France
alexandre.leblanc@univ-artois.fr, antoine.lavie@univ-artois.fr

Abstract: Membrane-type acoustic metamaterials have received much attention for low-frequency sound manipulation, especially in the form of decorated membrane resonators. In this paper, such resonators are obtained using fused deposition modeling. Beyond the practical aspects provided by this manufacturing method, the low density of the flexible filament used increases their effectiveness. Indeed, the mass usually added to the membrane center can easily be divided into several disjoint elements. Using rotary inertia of the added structures, new peaks of efficiency in both absorption and normal transmission loss appear when compared to usual decorated membrane resonators.

[GM]
Date Received: September 27, 2016 **Date Accepted:** May 17, 2017

As society evolves, new technologies emerge. They should be considered to respond to persistent problems such as sound absorption at low frequencies. Three-dimensional (3D) solid prototyping printers are already used to obtain efficient sound diffusers, but still marginal for creating acoustic absorbers. In fact, the basic idea is based on using porous or fibrous material to get efficient sound absorbers.[1] In order to provide low frequency modal control, such absorbers tend to be too bulky.[2] However, composite materials have been proposed in recent years in response to the dual issue of efficiency and compactness.[3]

Recently, sub-wavelength absorbers have been proposed, particularly in the form of membrane-type acoustic metamaterials[4] (MAMs). These MAMs have shown efficient sound absorption in the low frequency regime.[5] To this end, decorated membrane resonators (DMRs) with tunable weights have been developed.[6–8] The core mechanism is to obtain a dissipative system through the elastic deformation of the membrane,[9] this latter being enhanced by the high energy density achieved through resonance (the high density regions being non-radiative). Yang *et al.*[10] demonstrated that the optimum absorption for a DMR is limited to 50% of the incident energy if the wave is incident from only one of its side, while coherent perfect absorption is obtained with another sound incoming from the opposite direction with the same intensity but opposite phase. Such mechanism is unrealistic in practical applications, so other strategies as achieving total absorption by hybridizing two DMR resonances through the application of a thin gas layer are carried out (using multiple scattering generated by a back reflecting surface).[11] The deep-subwavelength scale of such cavity provides robust impedance matching and performs as a point acoustic sink in the vicinity of the DMR's anti-resonance.[10] The very narrow absorption bandwidth can be advantageous in frequency-selective applications but it could be also interesting to expand or increase the occurrence of absorption peaks, especially for sound insulation purpose.[12]

In this work, we show that by using split rings, DRM's efficiency could be strongly improved by the motion of its added elements. First, we propose few DRM designs which are easily produced with 3D printing. Then, we highlight their acoustic performances using experimental measures and numerical simulations.

Figure 1(a) presents the geometric definitions of the MAMs, the membrane radius is set to 50 mm in order to be easily mounted in a Brüel & Kjær impedance tube. These are obtained by a fused deposition modeling machine (MakerBot Replicator 2) using Ninjaflex (Ninjatek, Manheim, PA) flexible filament ($\rho = 1200\,\mathrm{kg/m^3}$, $E = 13.2\,\mathrm{MPa}$). The first investigated DMR is made with a central mass of 1.5 g (which

[a]Author to whom correspondence should be addressed.

defines the platelet radius $r_p = 10\,\text{mm}$ and its height $h_p = 4\,\text{mm}$), while the membrane itself weighs four times heavier. Here, the study of inertial effects of additional structures is privileged over other phenomena (e.g., mode hybridization), thus the ratio between the platelet and the membrane masses is deliberately chosen low. 3D-printed DMRs are evaluated with an impedance tube by the four-microphone transfer matrix method (ASTM E2611-09). Based on these experimental results, preliminary numerical studies, using finite element method (FEM), have also verified by using a correlation procedure the reasonable assumption of a constant damping, defining an isotropic structural loss factor.[13] Furthermore, the prestresses ($\sigma \approx 0.35\,\text{MPa}$) of the 3D-printed membranes used in the numerical simulations, mainly due to direct mounting on the impedance tube, are determined following the method derived by Wen *et al.*[14]

Figure 1(b) shows a rather good agreement between the measured normal transmission loss (TL_n) and the results of the numerical model using the above assumptions. Averaging the membrane displacements results in three null displacements at 100, 180, and 260 Hz. The first and third ones correspond to absorption peaks while the second conforms to the TL maximum value. The first FEM application depicted in Fig. 2 deals with the potential benefits that 3D printing can bring on MAM performance. Nowadays, pasting a small metal disk on a membrane can be considered as part of a usual procedure, even if the adhesion of this mass can quickly become a problem. However, this process is time consuming, and often provides a low lifetime object. Moreover, it does not make it possible to consider studying more complex structures. For the base DMR, in the investigated frequency range (80–1000 Hz), four absorption peaks are obtained with identical values for both the composite DMR and a printed membrane of a single flexible material (despite a platelet 6 times higher). On the contrary, splitting the platelet in 12 equally spaced parts (placed accordingly to the same outer radius $r_p = 10\,\text{mm}$) results in very differentiated performances. In Fig. 2, the fully flexible MAM benefits the most from this layout: an optimal absorption peak is observed at 150 Hz. This corresponds to the frequency for which the membrane vibration is maximum on the ring defining the position of the platelets [cf. Fig. 2 (b)],

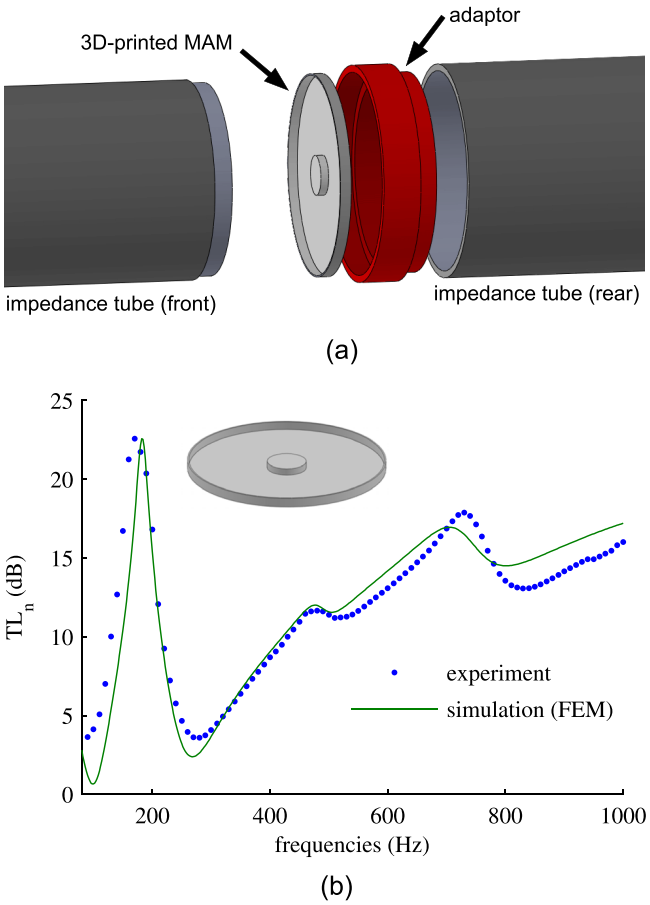

Fig. 1. (Color online) (a) Mounting a 3D-printed MAM on an impedance tube (Brüel & Kjær type 4206 or 7758). (b) Normal TL for the base DMR: the solid (respectively, dotted) line shows the calculated values (respectively, experimental measures).

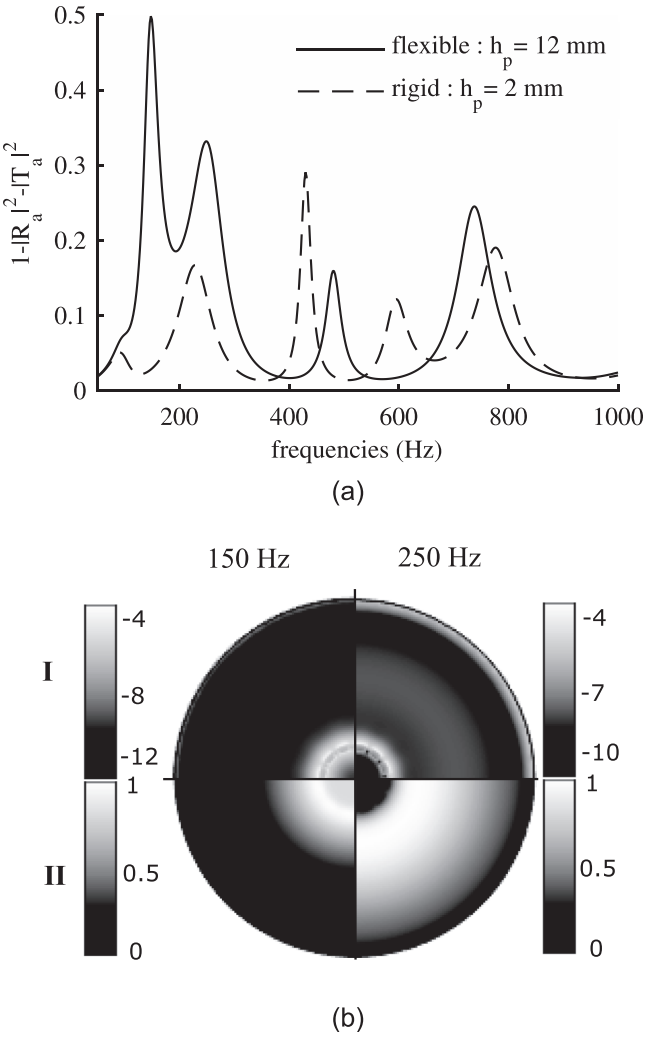

Fig. 2. (a) Predicted (FEM) absorption coefficient of the DMR with a split platelet. The solid lines are for the fully flexible MAM, while the dashed lines reflect the case where the added masses are rigid materials such as steel. (b) Fully flexible MAM I: distributions of the elastic potential energy density (log-transformed values); II: total displacements (adimensioned) within the membrane plane.

i.e., when the rotary inertia of the structures is maximized. Thus, high absorption is achieved through the flapping motion of those structures.[4] Here, the energy density in the perimeter region of the elements of the split platelet is larger by several orders of magnitude than everywhere else in the membrane. Thereby, a strong local dissipation is achieved, bringing an absorption peak (the flapping motions of the split platelet coupling only minimally to the radiation modes). At 250 Hz, this energy density is still around the outer perimeter of the elements, but, as the maximum vibration amplitude moves away from these structures, the predominant absorption mechanism is that of an average zero displacement of the whole membrane. Also, as two null averaged normal displacements are introduced by this phenomenon, an additional TL peak appears at 130 Hz while the original optimum [cf. Fig. 1(b)] is shifted by 20 to 200 Hz. Indeed, the energy required to rotate the attached masses is not radiated downstream of the DMR, and thus a new peak in both the absorption and TL curves appears. Also, a parametric numerical analysis has revealed that the choice of the number of the split platelet parts (here 12) did not significantly affect the performance of the MAM. However, a small frequency shift can be observed (e.g., +15 Hz between a 4 and a 12 parts split platelet and only for the first peak) due to the local stiffness distribution (the contact surface increases while the number of elements is decreased).

Two *structured membranes* (base DMR with an additional structure) are characterized in Fig. 3(a) via their TL. The first involves a flexible ring (outer radius $r_o = 26$ mm and inner radius $r_i = 24$ mm, with a height of $h_r = 4$ mm for a weight of 1.5 g). The first two peaks are located near the DMR ones, while the third is shifted from 100 Hz to high frequencies. Using another mass distribution as previously shown in Fig. 2, only the first peak is conserved in position (height is adapted to retain the

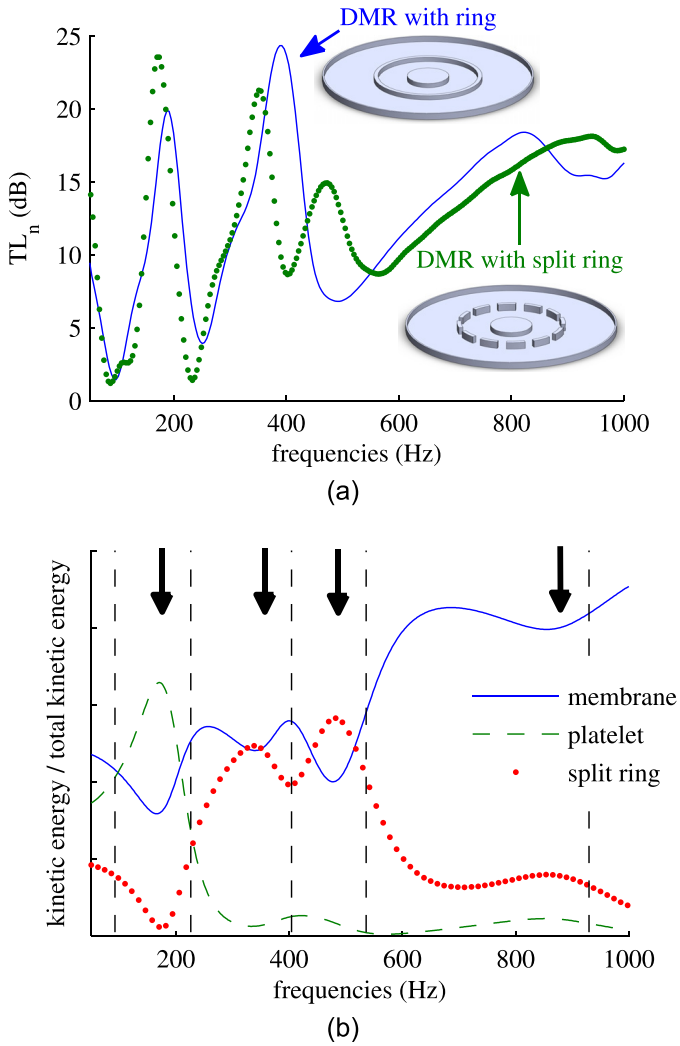

Fig. 3. (Color online) (a) TL at normal incidence for 3D-printed MAMs. The solid line represents the fully flexible MAM consisting of the base DMR with an additional ring. The dotted line shows the same DMR but with a split ring (with a height adjusted to maintain the same mass). (b) Kinetic energy distribution in the MAM components. The vertical dashed lines indicate the frequencies for which the average displacement of the membrane tends to zero while the arrows locate TL peaks.

same total weight, thus $h_r = 6\,\text{mm}$). Now, two peaks are located close to the original DMR absorption mode. Numerical simulations performed on the same structured membrane but with a rigid split ring (steel: $\rho = 7850\,\text{kg/m}^3$, $E = 200\,\text{GPa}$, $\nu = 0.33$; thus $h_r = 0.9\,\text{mm}$) have revealed that these modes are no longer present in this configuration. Indeed, for the base DMR, the membrane's maximum amplitude of the second peak (around 500 Hz) is located at the location of the ring radius. Thus, using a ring has a marginal impact on vibrational properties of the base DMR, acting only as a concentrated mass on the surface defined by the junction of the membrane and the ring. Again, this is not a valid assumption for the *split ring* case as the maximum kinetic energy density can be now located on the edge of the split ring elements. The influence of such specific dynamic motion on the membrane displacements (so its acoustic properties) is illustrated in Fig. 3(b). In this figure, the normalized kinetic energies for the three MAM components (membrane, central mass, and split ring) are drawn, indicating the TL peaks [cf. Fig. 3(a)] and membrane's displacements with null average. TLs are dependent on the ability of the membrane to transmit its energy to its structures while the absorption can benefit from the strong bending of the structures as an additional zero mean displacement appears in the vicinity of the new TL peak. Thus, and as Fig. 2 has shown for the simple split platelet case, using structures with small surface contact with the membrane but with a high moment of inertia can drastically improve the MAM performances.

In conclusion, we have demonstrated the possibility of using a 3D-printed MAM for low sound attenuation. This study testifies that a basic fused deposition modeling 3D printer allows to obtain easily and quickly efficient MAMs, since the

assembly process generally required for obtaining a DMR (gluing, riveting, etc.) is avoided. Both numerical and experimental applications show similar results for composite and fully flexible DMRs. Moreover, a low density property of the flexible material can be employed to obtain additional structures with a higher moment of inertia. Compared to usual DMRs, this leads to new peaks of efficiency in both absorption and normal TL. Also, using rotary inertia of the added structures on a membrane is potentially more efficient to deal with diffuse fields.

References and links

[1]K. Sakagami, S. Kobatake, K. Kano, M. Morimoto, and M. Yairi, "Sound absorption characteristics of a single microperforated panel absorber backed by a porous absorbent layer," Acoust. Aust. **39**, 95–100 (2011).

[2]C. Lagarrigue, J. P. Groby, V. Tournat, O. Dazel, and O. Umnova, "Absorption of sound by porous layers with embedded periodic arrays of resonant inclusions," J. Acoust. Soc. Am. **134**, 4670–4680 (2013).

[3]Y. Wang, C. Zhang, L. Ren, M. Ichchou, M.-A. Galland, and O. Bareille, "Sound absorption of a new bionic multi-layer absorber," Compos. Struct. **108**, 400–408 (2014).

[4]J. Mei, G. Ma, M. Yang, Z. Yang, W. Wen, and P. Sheng, "Dark acoustic metamaterials as super absorbers for low-frequency sound," Nat. Commun. **3**, 756 (2012).

[5]Z. Yang, H. M. Dai, N. H. Chan, G. C. Ma, and P. Sheng, "Acoustic metamaterial panels for sound attenuation in the 50-1000 Hz regime," Appl. Phys. Lett. **96**, 041906 (2010).

[6]C. J. Naify, C.-M. Chang, G. McKnight, and S. Nutt., "Transmission loss and dynamic response of membrane-type locally resonant acoustic metamaterials," J. Appl. Phys. **108**, 114905 (2010).

[7]Y. Zhang, J. Wen, Y. Xiao, X. Wen, and J. Wang, "Theoretical investigation of the sound attenuation of membrane-type acoustic metamaterials," Phys. Lett. A **376**, 1489–1494 (2012).

[8]Y. Chen, G. Huang, X. Zhou, G. Hu, and C.-T. Sun, "Analytical coupled vibroacoustic modeling of membrane-type acoustic metamaterials: Membrane model," J. Acoust. Soc. Am. **136**, 969–979 (2014).

[9]M. Yang, G. Ma, Y. Wu, Z. Yang, and P. Sheng, "Homogenization scheme for acoustic metamaterials," Phys. Rev. B **89**, 064309 (2014).

[10]M. Yang, G. Ma, Z. Yang, and P. Sheng, "Subwavelength perfect acoustic absorption in membrane-type metamaterials: A geometric perspective," Eur. Phys. J. Appl. Metamat. **2**, 10 (2015).

[11]G. Ma, M. Yang, S. Xiao, Z. Yang, and P. Sheng, "Acoustic metasurface with hybrid resonances," Nat. Mater. **13**, 873–878 (2014).

[12]X. Wang, H. Zhao, X. Luo, and Z. Huang, "Membrane-constrained acoustic metamaterials for low frequency sound insulation," Appl. Phys. Lett. **108**, 041905 (2016).

[13]A. Ba, A. Lavie, and A. Leblanc, "Soft 3d printed membrane type-acoustic metamaterials," in *Proceedings of the 23rd International Congress on Sound & Vibration*, Athens, Greece (2016).

[14]K.-T. Wan, S. Guo, and D. A. Dillard, "A theoretical and numerical study of a thin clamped circular film under an external load in the presence of a tensile residual stress," Thin Solid Films **425**, 150–162 (2003).